Nutrafoods (2024) 1 568-580 DOI 10.17470/NF-024-0066

Original Research

Protective mechanism of butyrate and palmitoylethanolamide highlighted by VitroScreen ORA® - a new microphysiological system mimicking colon inflammation

Marco Valente[1*]

Francesca Rescigno[2]

Stefano Francescato[1]

Sonia Facchin[3]

Edoardo Savarino[3]

Giovanni Baratto[1]

[1] Food Supplements R&D, Unifarco S.p.A., Santa Giustina, Italy

[2] VitroScreen, Milan, Italy

[3] Department of Surgery, Oncology and Gastroenterology (DISCOG), University Hospital of Padua, Padua, Italy

*Corresponding author
Marco Valente
Email: marco.valente@unifarco.it
Tel.: +39 04371943715

Abstract

The incidence and prevalence of inflammatory bowel disease (IBD) continues to increase worldwide. Furthermore, a considerable fraction of individuals with IBD do not respond effectively to conventional treatments, suggesting a need for new therapeutic strategies. Butyrate and palmitoylethanolamide (PEA) are individually recognised for their protective effect on the gut epithelial permeability barrier. In this study, VitroScreen ORA™ intestinal 3D scaffold-free spheroids were used to mirror *in vitro* a model of an inflamed colonic epithelium and to investigate, in a preliminary setting, the protective mechanisms of a synergistic blend of butyrate and PEA. Spheroids were produced using human colonic fibroblasts and primary epithelial colonic cells. Differentiated spheroids were pretreated with either mesalamine, butyrate, PEA, or a blend of butyrate and PEA in a 3:1 ratio. To evaluate the protective effect of these molecules, a stimulation with interleukin 1β or with dextran sodium sulfate was applied to induce a pro-inflammatory status and epithelial damage respectively. ELISA assay and immunohistochemical techniques were used to detect the inflammatory status and epithelium integrity. Butyrate mitigated the expression and release of interleukin-1β while PEA increased zonula occludens-1 expression. Treatment with the blend consisting of butyrate and PEA showed a synergistic effect on tight junctions in terms of zonula occludens-1 increased expression and improved localization. Our preliminary data are promising, suggesting an application of ORA™ intestinal spheroids as an innovative platform with the ability to mirror gut inflammatory status. Furthermore, the results suggest a novel application of butyrate and PEA in clinical practice to better manage pathogenesis and flare-ups of IBD.

Keywords: 3D scaffold-free spheroids, inflammatory bowel disease, palmitoylethanolamide, butyrate, mesalamine, tight junctions

Introduction

Inflammatory bowel disease (IBD) includes chronic idiopathic disorders characterised by repetitive episodes of gut inflammation. Crohn's disease (CD) and ulcerative colitis (UC) represent two of the most common clinical forms of IBD and are differentiated by their location and depth of involvement in the bowel wall [1]. The prevalence of IBD differs by several sociodemographic aspects. It is much more prevalent in Western countries than in Asia or Africa. New data suggests that the incidence and prevalence of IBD is still increasing worldwide. Approximately 0.3% of the European population and 0.5% of the North American population have been diagnosed with IBD [2, 3].

Although the pathogenesis remains unknown, it has been hypothesized that IBD occurs in genetically susceptible individuals. There is also convincing evidence to implicate immunological and environmental factors. Some data suggests that heightened gut permeability plays a key role in the pathogenesis of IBD [4]. IBD has been associated with poor quality of life and often results in complications, including hospitalizations and surgical procedures [5, 6].

There are two main challenges in the therapeutic management of IBD: induction of a response and maintenance of the remission. Conventional treatments focus on the management of symptoms through pharmacotherapy, including aminosalicylates, corticosteroids, immunomodulators, and biologics, with other general measures and/or surgical resection if necessary. However, a considerable number of individuals with IBD do not respond to available treatments or lose response over time, suggesting a need for new therapeutic strategies [7].

Butyrate, a short-chain fatty acid (SCFA) produced by bacterial fermentation of dietary fibres, plays a key physiological role in maintaining the health and integrity of the intestinal mucosa by regulating the balance between epithelial cell proliferation, differentiation and apoptosis [8]. It has been found that individuals with IBD have reduced levels of well-known butyrate-producing bacteria in the gut [9]. In view of this, some research groups have proposed oral butyrate supplementation as a nutraceutical product to reach clinical improvement/remission in individuals with IBD, proving the safety and effectiveness of this SCFA [8]. Butyrate has well-documented intestinal effects on IBD. It acts by several mechanisms, such as reinforcing the colonic defensive barrier by increasing production of mucins and decreasing intestinal epithelial permeability by increasing the expression of tight junction (TJ) proteins [10, 11].

Butyrate also has anti-inflammatory effects. By inhibiting the histone deacetylase activity (HDAC) that leads to hyperacetylation of histones with suppression of nuclear factor kappa B (NF-kB) in activated B cells, butyrate can lead to activation and stimulation of histone acetyltransferases activity, influencing several cellular processes, including cell chemotaxis, differentiation, proliferation, apoptosis and modulation of oxidative stress [12].

Palmitoylethanolamide (PEA) is an endocannabinoid-like lipid mediator with extensively documented anti-inflammatory, analgesic, antimicrobial, immunomodulatory and neuroprotective effects [13–18]. Synthesized on demand within the lipid bilayer, it acts locally and is found in all tissues, including the gut. PEA is thought to be produced as a pro-homeostatic protective response to external stressors that trigger inflammation, neuronal damage and pain tissue injury. Therefore, the endogenous production of PEA is usually upregulated in disease conditions [19]. However, in chronic inflammation, protracted stimulus may cause a decrease in local PEA content. Exogenous administration of PEA as a nutraceutical product could be advantageous to restore appropriate endogenous levels and to support its natural

protective, anti-inflammatory and analgesic effects [20–22]. Proposed direct or indirect targets for PEA actions include cannabinoid (CB)1 and CB2 receptors, transient receptor potential vanilloid type-1 (TRPV1) ion channels and peroxisome proliferator-activated receptor (PPAR) α, which are involved in the pathways controlling intestinal inflammation. An increasing number of studies have highlighted the benefits of exogenous administration of PEA for the management of IBD thanks to its ability to attenuate inflammation and intestinal permeability and to stimulate colonic cell proliferation [18].

In our research study, the complexity of intestinal colonic architecture was reproduced by tissue engineering (TE) that aimed to generate a miniaturized intestinal scaffold-free spheroid system by self-assembly in hanging drops of primary human colonic stromal fibroblasts and primary human epithelial colonic cells in a sequential co-culture. This approach allowed us to recapitulate a stromal core surrounded by epithelial cells with strong cell-matrix interactions. Thanks to a TE bottom-up approach and to the 3D configuration, primary cells at early passages can faithfully preserve the physiological phenotype, reproducing a complex and self-organized Micro Physiological System (MPS) where tissue guidance, topographical signals, native cell-cell interactions, and cell-matrix interaction are mimicked well. After spontaneous cellular self-assembly, scaffold-free intestinal spheroids were cultured for 10 days to allow for cellular stabilization and differentiation. VitroScreen ORA™ intestinal 3D scaffold-free spheroids were applied to this preliminary research project with the aim of mirroring *in vitro* a model of an inflamed colonic epithelium induced by interleukin 1β (IL-1^{2}) exposure and by dextran sulfate (DSS), which is a known key inducer of colitis and intestinal barrier impairment [23, 24] (both directly dosed in the colonic spheroids culture media). We also aimed to investigate the protective mechanisms of butyrate and mesalamine compared with a synergistic blend of butyrate and PEA. This multiple primary endpoints approach involved readout parameters of the protein expression and localization by immunohistochemistry and biochemical assays.

Material and methods

Cell source and culture

Primary human colonic fibroblasts (HCoF) and primary epithelial colonic cells (HCoEPIC) were purchased from Innoprot (Derio, Spain), seeded on a poly-L-Lysine coating (2 mg/cm^2), cultured and amplified at early passages in Fibroblast medium and HCoEPIC medium (Innoprot, Derio, Spain), respectively to obtain approximately 20 × 106 cells.

VitroScreen ORA™ intestinal model production and inflammatory status induction

HCoF and HCoEPIC were detached when 90% confluence was reached. To develop an ORA™ intestinal model, a sequential co-culture was performed according to VitroScreen internal procedure as described in the international publication WO/2019/092667 A1 (patents.google.com/patent/WO2019092667A1/en). Spheroids were produced using HCoF that were first detached, washed twice with DPBS 1X (Merck Life Science S.r.l., Milan, Italy) and incubated with Trypsin/EDTA (TE) solution (Primary Detach Kit, Innoprot, Derio, Spain) for 5 minutes. Cells were counted, centrifuged and seeded in Akura®Pate (InSphero AG, Schlieren, Switzerland) by ViaFlo Assist Plus (Integra Bioscience AG, Zizers, Switzerland) in order to obtain 8,000 cells/spheroids. Using the hanging drop technique, specific geometrical guidance allowed cells to self-assemble and aggregate, forming round-shaped tridimensional scaffold-free spheroids. After 3 days in the hanging drop system, intestinal colonic stroma was well formed, and spheroids

were ready for HCoEPIC seeding. HCoEPIC were detached, washed twice with DPBS 1X (Merck Life Science S.r.l., Milan, Italy) and incubated with TE solution (Primary Detach Kit, Innoprot, Derio, Spain) for 5 minutes. Cells were counted (2,000 cells/spheroids), centrifuged and seeded in hanging drops of colonic spheroids to obtain intestinal spheroids of 10,000 cells/each. Once assembled, ORA™ spheroids were transferred into Akura 96 V2® plate (InSphero AG, Schlieren, Switzerland). Tissues were cultured in this configuration for an additional 10 days in order to allow cell stabilization and intestinal epithelial differentiation with specific 3D architecture. On ORA™ spheroids the pro-inflammatory state was induced by exposure to IL-1β (human recombinant, Merck Life Science S.r.l., Milan, Italy) 10 ng/mL for 24 hours. After 24 hours of stimulation, fresh culture media was added to allow IL-1β elimination and to avoid interference with endogenous IL-1β dosed in the culture media. The barrier damage was induced by exposure to DSS, a molecule that is well-known to induce UC in mice. DSS was added to the culture medium at 3% for 72 hours. Triplicate of culture media and samples (20 pooled spheroids/each replicate) were collected for ELISA assay and whole mount immunofluorescence staining. The final 3D configuration of the ORA™ intestinal model is shown in **Fig. 1**.

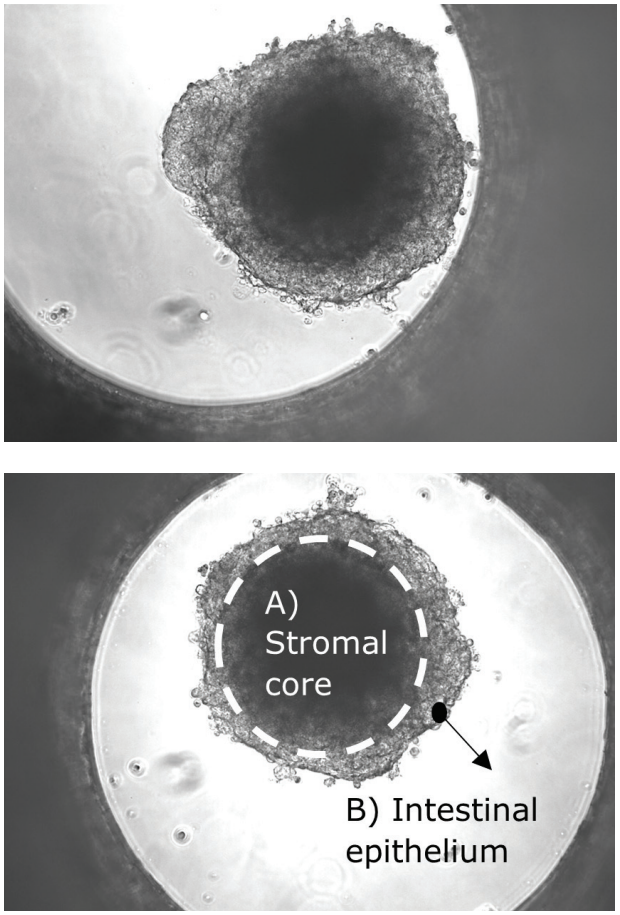

Figure 1 VitroScreen ORA™ intestinal spheroids.
(A) internal colonic stromal core;
(B) Intestinal epithelium surrounding the stroma.
A stromal core (white circle, A) is visible inside the 3D spheroids surrounded by the epithelial compartment (black arrow, B).
Brightfield microscope acquisition 10× mag.

ATP assay for cell viability detection

ATP measure is used as an indicator of metabolic activity and to identify a potential toxic effect. It was performed on ORA™ intestinal spheroids by 3D CellTiter Glo Luminescent Cell Viability (Promega, Madison, WI, USA) using Adenosine-5-triphosphate (ATP) quantification. The assay procedures include the addition of a single reagent directly to tissues cultured in medium. The cell lysis and the generation of a luminescent signal was proportional to the amount of available ATP. A luminescence reader can detect a stable luminescent signal 30 minutes after the reagent is added and mixed.

ELISA assay for quantification of released IL-1β

The enzyme-linked immune-absorbent assay (R&D Systems, MN, USA) is a test based on the specific recognition of an antigen by an antibody. The accuracy of the spectro-photometrical measurements was in the 0–2 optical density (OD) range: < +/- (1% + 10 mean OD). The raw data of OD were directly recorded in the Microplate autoreader (TECAN INFINITE M-200) further processed by Software iControl and reported in an Excel file. The biological replicate OD has been interpolated in the concen-

tration-OD curve of hIL-1β standards (0 pg/mL, 3.9 pg/mL, 7.8 pg/mL, 15.6 pg/mL, 31.3 pg/mL, 62.5 pg/mL, 125 pg/mL, and 250 pg/mL) to calculate the IL-1β concentration in the samples. If one sample, whether treated with negative control or with positive control, was outside the sensitivity range (<1 pg/mL), the results were reported as <3.9 pg/mL or >250 pg/mL.

Immunofluorescence staining for zonula occludens-1 (ZO-1)

VitroScreen ORA™ intestinal model DSS-exposed series (w/o treatments), were collected for histological analysis to evaluate the effect on barrier function integrity by detection of ZO-1 expression and localization. Tissues were washed in PBS 1× and fixed in formalin buffered solution 10% (Merck Life Science S.r.l., Milan, Italy) for 1 hour at room temperature. After tissue fixation, samples were prepared for histological clearing before incubation with the primary antibody. Visikol Histo-M Starter Kit® (Visikol, Hampton, NJ, USA) was used as a clearing reagent and samples were treated according to internal procedure: pooled samples (*n*=10/each pool) were dehydrated and rehydrated in cycles of 15 minutes by incubations with increasing concentrations of ET-OH solutions (from 50% to 100%). After permeabilization with PBS-Triton solution 0.2% and Visikol Histo® Permeabilization Buffer (Visikol, Hampton, NJ, USA), the blocking of specific sites was performed by incubation with Visikol Histo® Blocking Solution (Visikol, Hampton, NJ, USA). Samples were incubated with ZO-1 rabbit polyclonal primary antibody (HPA001636, Merck Life Science, dilution: 1:500) overnight at 4°C. Alexa 555 donkey anti-rabbit and Alexa 488 goat anti-mouse (Life Technologies, at appropriate dilutions) were used as a secondary antibody while nuclei were stained with DAPI (Merck, 1:2500). Stained intestinal spheroids were cleared with Visikol Histo®-M overnight at 4°C. The acquisitions were performed by Leica THUNDER DMi8 3D Cell Imager and Z-stacks video was acquired with a Leica sCMOS Camera and post-processed by LASX 3.0.1 software (Leica Microsystems Srl, Milan, Italy). Z-stacks were acquired to observe the whole volumes of 3D spheroids. Signal expression acquisition was optimized by the Large Volume Thunder Computational Clearing (LVCC) algorithm and some more informative optical planes were extrapolated from the Z-stack video. For the efficacy study, the ZO-1 expression signal was quantified by Leica LASX software Leica (Microsystems S.r.l., Milan, Italy) on 2D maximum projection images, derived from each Z-stacks to quantify the intensity of expression signal on whole 3D samples, considering the contribute of all focal planes.

Model Induction and gut spheroids treatment

After 10 days of culture, and once completely differentiated, spheroids were pretreated within 48 hours with either mesalamine 20 mM (Merck Life Science S.r.l., Milan, Italy), sodium butyrate 6 mM (Unifarco SPA), PEA 6 mM, (Unifarco SPA) or with butyrate and PEA blended in a 3:1 ratio, added to the culture medium. After 48 hours, the media were changed, and a direct inflammatory stimulus was performed by exposure to IL-1β 10 ng/mL for 24 hours to evaluate the inflammatory status of ORA™ spheroids. After 24 hours of stimulation, all media were discarded, and fresh media were added to the culture, avoiding interference of residual IL-1β and the endogenous IL-1β released after stimulation. To simulate the barrier damage, another series was stimulated with DSS 3%, which was added within 72 hours. At the end of all stimulation, culture media of all series were collected for ELISA assay and whole mount immunofluorescence.

Results

The statistical analysis was performed by one way- ANOVA (** p< 0.01, *** p< 0.005).

Cell viability

In order to evaluate the non-toxic dose at the defined exposure ATP, quantification was performed on the intestinal spheroids series after treatment with DSS and IL-1β compared with untreated negative control (NC). In **Fig. 2** the percentage (%) of viability was reported compared with NC=100%. The safe and non-toxic doses for all compounds were chosen after a preliminary cytotoxicity assay (data not shown).

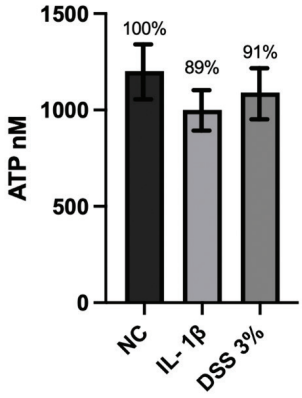

Fig. 2 Metabolic activity evaluated by ATP assay. Negative Control (NC) compared with treated samples (individual biological replicates n=6). Each series was exposed for a defined time to the inducers.

As shown in **Fig. 2**, the different treatments did not severely affect cellular viability and metabolic activity of intestinal spheroids with values close to untreated controls (89%, 91% and 100%, respectively).

Release of IL-1β by spheroids

Quantification of IL-1β release dosed in the culture media by ELISA assay was used to confirm the pro-inflammatory state of spheroids induced by exogenous IL-1β and DSS 3% exposure (separate series). The profile of endogenous IL-1β release is reported in the **Fig. 3**.

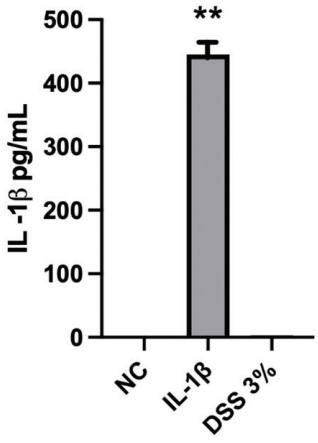

Fig. 3 IL-1β quantification on intestinal ORA™ spheroids. (<1 pg/mL sensitivity range). ** p< 0.01 (by one-way ANOVA).

As observed in the **Fig. 3**, exposure to DSS did not detect a significant release of the targeted pro-inflammatory cytokine. On the contrary, the direct inflammation of intestinal ORA™ models with IL-1β 10 ng/mL allowed the highest cytokine amount in the culture media (445 pg/mL) during 24 hours of exposure (and an additional 24 hours of recovery without stimulation).

Inflammatory response modulation

ORA™ intestinal spheroids were cultured for 10 days to allow complete tissue differentiation. They were pretreated for 48 hours with either sodium butyrate (SB) 0.6 mM, PEA 0.6 mM or a blend of both in a 3:1 ratio (MIX), before exposure to pro-inflammatory cytokine. Mesalamine 20 mM was employed as reference compound. After 48 hours of pretreatment, intestinal spheroids were exposed to IL-1β 10 ng/mL for 24 hours. After 24 hours of stimulation, media was discarded to avoid exogenous IL-1β interference. After an additional 24 hours of recovery, endogenous IL-1β release was quantified in the culture medium to evaluate the efficacy of sodium butyrate and/or PEA in counteracting inflammation as a result of cytokine exposure. **Fig. 4** shows the IL-1β trend following pretreatment with direct exposure to IL-1β cytokine and with sodium butyrate and/or PEA.

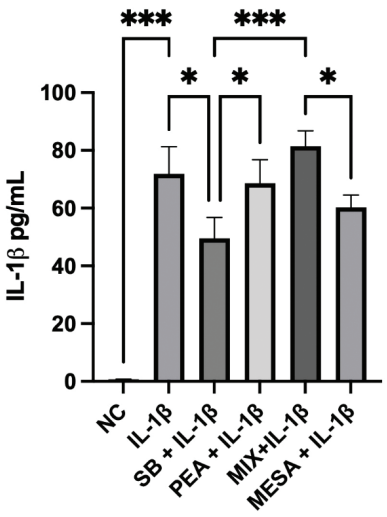

Fig. 4 IL-1β quantification on ORA™ intestinal model in evaluating efficacy of nutraceuticals. (<1 pg/mL sensitivity range). ** p< 0.01 (by one-way ANOVA).

Pro-inflammatory induction by exposure of treated spheroids to IL-1β 10 ng/mL for 24 hours led to an increase in cytokine production compared with untreated samples, which confirmed the response observed in the preliminary data. Pretreatment with sodium butyrate 0.6 mM for 48 hours SB+IL-1β series) showed a positive effect in reducing IL-1β release (p<0.05) compared with samples that were not pretreated, suggesting a protective effect against direct pro-inflammatory induction. Pretreatment with PEA (PEA+IL-1β series) 0.6 mM and with the sodium butyrate and PEA blend for 48 hours (MIX-+IL-1β series) did not show the same protective effect against inflammation, with values close to those for inflamed and untreated samples (68.5 pg/mL and 81.46 pg/mL, respectively). Pretreatment with mesalamine 20 mM for 48 hours (MESA+IL-1β series) reduced the IL-1β release if compared with PEA and blend exposure, due to a preventive anti-inflammatory activity. Of all treatments, sodium butyrate showed a specific early anti-inflammatory effect.

Evaluation of TJ structure modification after inflammatory status induction by immunofluorescence for ZO-1

Differential localization and expression were followed by whole mount immunofluorescence for the main TJ protein ZO-1: 3D spheroids were challenged by direct exposure to IL-1β and DSS for barrier function impairment compared with the untreated series. **Fig.5** shows the main optical plane for each experimental condition extrapolated from 3D Z-stacks.

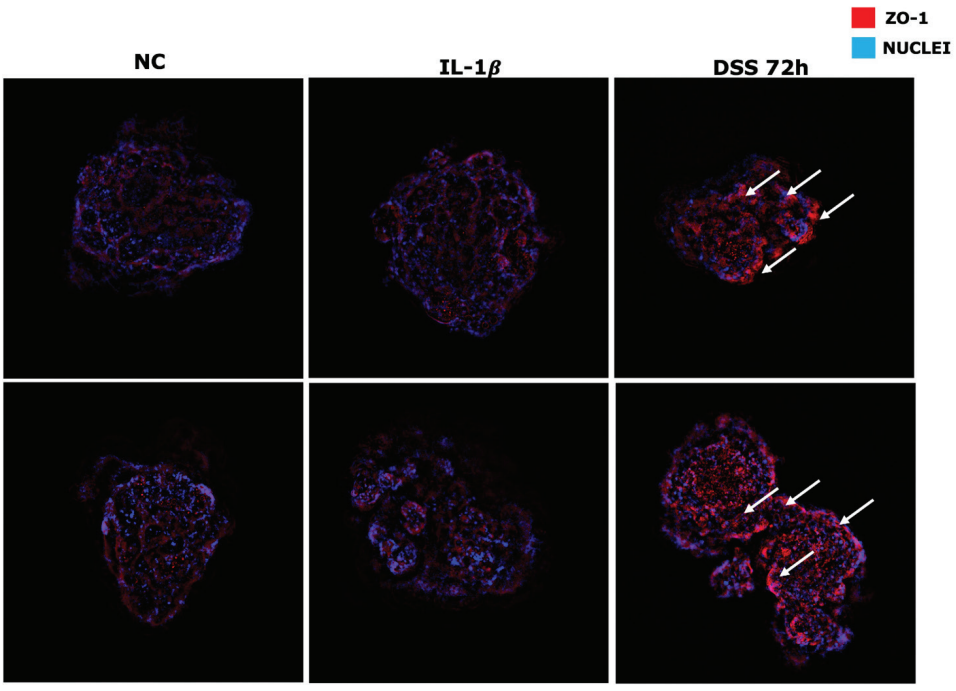

Figure 5 Whole mount ZO-1 Immunofluorescence in 3D. Main optical planes are reported from 3D Z-Stack.
DSS and indirect induction with IL-1β showed a very similar ZO-1 pattern (white arrows). 20× mag.

Untreated (NC) and inflamed series induced by exposure to IL-1β 10 ng/mL did not show visible differences in terms of ZO-1 intensity signal and protein localization. Exposure to DSS led to an increase of ZO-1 expression as a defence mechanism with a cytoplasmatic localization. The evaluation of barrier function of butyrate and/or PEA was conducted by ZO-1 expression analysis. Immunofluorescent images extrapolated from 3D Z-stacks are reported in **Fig. 6.**

Despite no significant differences observed between NC, DSS and SB + DSS series in terms of signal quantification, red signal associated to ZO-1 protein in untreated samples (NC) appeared linear and continuous, and diffused among cells. Exposure to DSS revealed a slight difference in terms of intensity and localization, showing a spotted signal inside and around cells. Pretreatment with sodium butyrate for 48 hours revealed a slightly increased ZO-1 signal, and the point-like localization becomes more pericellular, suggesting a possible protective role on barrier integrity. A similar configuration was also observed for PEA pretreated tissues (PEA+DSS series). Pretreatment with the blend led to a more evident signal increase and a recovery of point-like localization surrounding nuclei inside the greater focal planes, with a configuration very close to mesalamine pretreated series. Pretreatment with PEA preserved and increased ZO-1 expression with higher values if compared with a sodium butyrate effect. Sodium butyrate and PEA blended in a 3:1 ratio (SB+DSS and MIX+DSS series) showed the highest effect in terms of zonulin expression, with values overlapping to mesalamine stimulation. A signal quantification was performed, and the results are shown in **Fig. 7**.

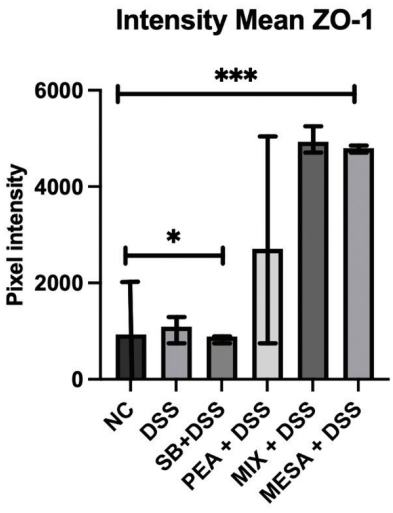

Figure 7 ZO-1 signal quantification on intestinal ORA™ intestinal model in evaluating efficacy of nutraceuticals. * $p < 0.05$, *** $p < 0.0001$ (by one-way ANOVA).

Figure 6 ZO-1 expression by whole mount immunofluorescence on intestinal ORA™ intestinal model treated and exposed to DSS 3%. 20× mag.

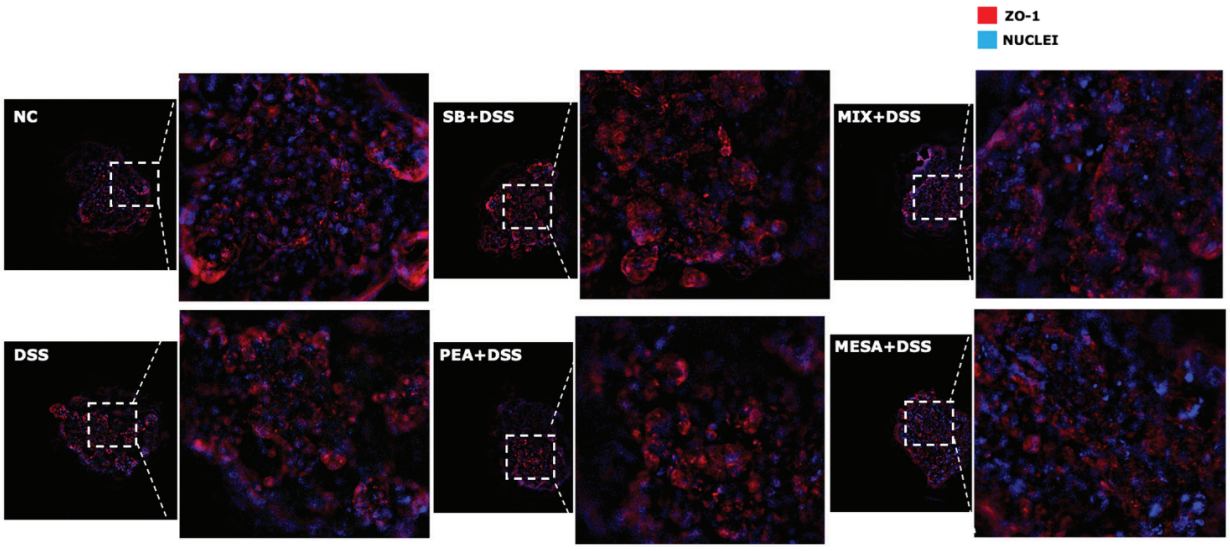

Discussion

Cellular viability by ATP

In the adopted experimental conditions, treatment with DSS did not affect the metabolic homeostasis of intestinal spheroids (**Fig. 2**). This result is in line with previous data generated on Caco-2 systems [25–27].

Quantification of IL-1β release

As expected, and according to literature on simplified intestinal cells systems such as Caco-2 [28], as a preliminary starting point, the exposure of intestinal spheroids to a pro-inflammatory stimulus induces a significant release of IL-1β compared with untreated control (**Fig. 4**). This data suggests that ORA™ intestinal spheroids could be susceptible to pro-inflammatory induction and that the stimulus goes over the induction time (up to 48 hours). Pretreatment of spheroids with sodium butyrate showed a protective effect against pro-inflammatory stimulus, which is in agreement with literature findings [29, 30]. Since butyrate acts as a barrier protection agent against inflammatory insults, we presume that this SCFA works as an effective molecular shield protecting epithelial cells. The hypothesis of a preventive role of this compound is also corroborated by Magnusson *et al.* [31] who demonstrated that expression of inflammatory pathways could be more effectively downregulated by butyrate in non-inflamed colonic biopsies of individuals with UC than in inflamed ones. On the one hand, a weaker response of inflamed gut to butyrate could depend, at least in part, on downregulation of gene encoding enzymes involved in butyrate metabolism and oxidation. On the other hand, during gut inflammation, it is well known that crypts lose physiological architecture [32, 33]. This phenomenon exposes stem cells located in the bottom of crypts to the luminal butyrate, which could inhibit proliferation of undifferentiated cells because of butyrate-paradox [34]. In order to avoid a delayed wound repair, it would be reasonable to evaluate the use of low doses of butyrate during the acute phase of IBD. Overall, these data suggest that butyrate supplementation may contribute effectively to the induction of disease remission and even sustain it over time. Thus, butyrate can play a role against the activation of immune-mediated response, interrupting the vicious circle that characterizes gut barrier damage in intestinal inflammatory diseases. Mesalamine, the chosen anti-inflammatory reference compound, reduced the spheroids secretion of IL-1β. However, it is interesting to note that sodium butyrate appears more effective than mesalamine because the concentration of sodium butyrate applied on spheroids is 30 times lower than that of mesalamine. Based on this evidence, we speculate that the human colonic epithelium is more responsive to sodium butyrate compared with mesalamine, supporting the use of butyrate in gastroenterology to prevent gut inflammatory conditions and to better manage acute and remission phases of IBD. However, neither pretreatment with PEA alone nor PEA mixed with sodium butyrate seem to have an influence on IL-1β release. These results, which appear to contradict the known anti-inflammatory activity of PEA, could be explained by the absence of submucosal cells in our spheroid model. Submucosal cells, such as dendritic cells, mast cells and macrophages are generally highly responsive to PEA [13]. Furthermore, it has been reported that the expression of some PEA receptors in the colonic epithelium increases only during inflammatory events [35]. Therefore, in our experimental setting based on a pretreatment of healthy spheroids, the colonic epithelium may not express significant levels of PEA receptors such as to ensure a local anti-inflammatory response. Likewise, pretreatment with PEA and sodium butyrate did not seem to trigger a protective effect against inflammation. The reason

why PEA seems to neutralize the benefits of butyrate in this *in vitro* model remains to be ascertained. Although further investigations are needed, it is possible to hypothesize that both sodium butyrate and mesalamine act by a protective mechanism on colonic epithelium while PEA properties cannot be investigated in our experimental conditions.

ZO-1 expression and localization

As reported in **Fig. 6**, ZO-1 protein localization appeared linear, continuous and diffused among cells in untreated samples (NC series). In contrast, exposure to DSS showed a spotted signal inside and around cells, which suggests a barrier impairment. The point-like ZO-1 signal became more pericellular in spheroids pretreated with butyrate, with a similar pattern observed for PEA treated tissues (PEA+DSS series). Moreover, pretreatment with the blend of butyrate and PEA (MIX + DSS) led to a more evident signal increase and a recovery of the physiological protein localization with greater focal planes, and with a configuration very close to the mesalamine pretreated series (MESA + DSS). These data suggest a sort of protective role of butyrate and PEA on barrier integrity. In **Fig. 7** ZO-1 signal quantification is reported: untreated and DSS exposed tissues did not show visible differences in terms of ZO-1 intensity signal and protein localization. No significant signal intensity differences were observed between NC, DSS and sodium butyrate plus DSS series (SB + DSS). On the contrary, pretreatment with PEA was associated with a significant increase of ZO-1 expression. At the same time, the blend of sodium butyrate and PEA (MIX + DSS) showed the highest effect in terms of ZO-1 expression, with values overlapping those of mesalamine stimulation. In the adopted experimental conditions, DSS exposure does not induce a significant imbalance of ZO-1 expression in terms of signal intensity, although a slight shift of the cellular localization of ZO-1 was detected, suggesting a non-significant barrier damage. As previously reported on Caco-2 systems, DSS and other molecules known to induce epithelial damage (such as LPS, pro-inflammatory cytokines, pathogen bacteria, alcohol etc.) led to TJ remodelling and specifically to the mis-localization of ZO-1 through the inhibition of cell protein trafficking [36–39]. The biological effect associated with DSS cannot be described as a clear barrier integrity damage, as in most of papers, but as an early response of the colonic epithelium to recover an early attempt at barrier integrity, mirroring a proactive defence mechanism. Apparently, this result is in contrast with previous *in vitro* and *in vivo* findings in which the ZO-1 expression in gut mucosa decreased by DSS-treatment affecting the permeability [40–43, 25]. However, it should be noted that the effect of DSS on ZO-1 expression could be strongly influenced by the concentration of DSS employed in the experiment, duration of the treatment and above all the biological system. To the best of our knowledge, no papers have been published with the protocol adopted in this work. Within this framework, it is worth emphasizing that pretreatment with PEA increases ZO-1 expression. To the best of our knowledge, no previous work has highlighted a direct effect of PEA on colonic ZO-1 expression. Therefore, in view of the above, we speculate that PEA can enhance ZO-1 expression as an early defence mechanism by acting on PPARs or endocannabinoid receptors. Moreover, as previously reported, the blend of butyrate and PEA is more effective than PEA alone in increasing ZO-1 expression. For this reason, we could speculate that butyrate acts as an enhancer of PEA receptor expression.

Although these hypotheses need to be confirmed by further data, the interpretation of results is corroborated by previous studies. On the one hand, several data suggest that the anti-inflammatory and anti-hyperalgesic activities of PEA involve the activation of PPAR-δ

and PPAR-γ as well as PPAR-α [45]. Furthermore, Wächtershäuser *et al* demonstrated the ability of butyrate to upregulate PPAR-γ mRNA and protein in Caco-2 cells in a dose- and time-dependent manner [45]. On the other hand, it is well known that PEA targets transient receptor potential ion channels (TRPs) [46, 47, 18]. For instance, PEA can activate the TRPV1 receptor at the apical Caco-2 membrane, modulating permeability [48]. At the same time, in a model of kidney epithelial cells, butyrate seems to modulate TRPV1 activity in a dose-dependent manner as partial agonist. Interestingly, butyrate alone does not result in significant activation of TRPV1, however, preactivation of channels with capsaicin primes marked TRPV1 activation when butyrate is subsequently applied, regardless of whether capsaicin was still present [49]. In view of the above, we speculate that butyrate could contribute to amplify the effect of PEA on the ZO-1 expression. Although further studies are needed to clarify how butyrate exactly affects PEA properties, it is reasonable to suppose that PPARs and TRPs represent the crossroads in a signalling pathway where these two molecules interact.

Conclusion

VitroScreen ORA™ intestinal spheroids represent a new, ethical and advanced microphysiological system suitable for pre-clinical studies applied to nutritional ingredients mirroring both the morphological and biochemical features of inflamed gut epithelium. Overall, our preliminary results are encouraging. They demonstrate a protective role of sodium butyrate and PEA in gut barrier integrity and suggest the adoption of these nutraceuticals in clinical practice to better manage pathogenesis and IBD flare-ups. When taken together, all results pave the way for further investigations to gain a deeper understanding the molecular mechanism of action of butyrate and PEA alone on intestinal epithelium and the synergic combination of both by a multiparametric approach.

Conflicts of interest

M. Valente, S. Francescato and G. Baratto are employees of Unifarco S.p.A. a company that develops, manufactures and markets food supplements.

Edoardo Vincenzo Savarino has served as speaker for Abbvie, Agave, AGPharma, Alfasigma, Aurora Pharma, CaDiGroup, Celltrion, Dr Falk, EG Stada Group, Fenix Pharma, Fresenius Kabi, Galapagos, Janssen, JB Pharmaceuticals, Innovamedica/Adacyte, Malesci, Mayoly Biohealth, Omega Pharma, Pfizer, Reckitt Benckiser, Sandoz, SILA, Sofar, Takeda, Tillots, Unifarco; has served as consultant for Abbvie, Agave, Alfasigma, Biogen, Bristol-Myers Squibb, Celltrion, Diadema Farmaceutici, Dr. Falk, Fenix Pharma, Fresenius Kabi, Janssen, JB Pharmaceuticals, Merck & Co, Nestlè, Reckitt Benckiser, Regeneron, Sanofi, SILA, Sofar, Synformulas GmbH, Takeda, Unifarco; he received research support from Pfizer, Reckitt Benckiser, SILA, Sofar, Unifarco S.p.A, Zeta Farmaceutici.

Sonia Facchin has served as a speaker for Sila and Unifarco. She has served as a consultant for: Unifarco S.p.A., Sila, Zeta farmaceutici, Personal Genomics, BMR Genomics.

Funding

This study was co-funded by Unifarco and VitroScreen.

References

1. McDowell C, Farooq U Haseeb M (2023) Inflammatory Bowel Disease. In: *StatPearls*; Treasure Island (FL). Available at: https://www.ncbi.nlm.nih.gov/books NBK470312/ (Accessed 04/09/2023)

2. Dahlhamer JM, Zammitti EP, Ward BW, Wheaton AG, Croft JB (2016) Prevalence of inflammatory bowel disease among adults aged ≥18 years – United States 2015. MMWR Morb Mortal Wkly Rep 2016 Oct 28;65(42):1166–1169

3. Hammer T, Langholz E (2020) The epidemiology of inflammatory bowel disease: balance between East and West? A narrative review. Dig Med Res 3:48.

4. Fasano A (2008) Physiological, pathological, and therapeutic implications of zonulin-mediated intestinal barrier modulation. Am J Pathol 173(5):1243–1252

5. Soriano CR, Powell CR, Chiorean MV, Simianu VV (2021) Role of hospitalization for inflammatory bowel disease in the post-biologic era. World J Clin cases 9(26):7632–7642

6. Cohen RD (2002) The quality of life in patients with Crohn's disease. Aliment Pharmacol Ther 16(9):1603–1609

7. Actis GC, Pellicano R (2017) Inflammatory bowel disease: Efficient remission maintenance is crucial for cost containment. World J Gastrointest Pharmacol Ther 8(2):114–119

8. Sabatino A Di, Morera R, Ciccocioppo R, Cazzola P, Gotti S, Tinozzi FP, *et al* (2005) Oral butyrate for mildly to moderately active Crohn's disease. Aliment Pharmacol Ther 22(9):789–794

9. Machiels K, Joossens M, Sabino J, De Preter V, Arijs I, Eeckhaut V, *et al* (2014) A decrease of the butyrate-producing species Roseburia hominis and Faecalibacterium prausnitzii defines dysbiosis in patients with ulcerative colitis. Gut 63(8):1275–1283

10. Jung TH, Han KS, Park JH, Hwang HJ (2022) Butyrate modulates mucin secretion and bacterial adherence in LoVo cells via MAPK signaling. PLoS One17(7):e0269872

11. Peng L, Li ZR, Green RS, Holzman IR, Lin J (2009) Butyrate enhances the intestinal barrier by facilitating tight junction assembly via activation of AMP-activated protein kinase in Caco-2 cell monolayers. J Nutr 139(9):1619–1625

12. Silva JPB, Navegantes-Lima KC, Oliveira ALB, Rodrigues DVS, Gaspar SLF, Monteiro VVS, *et al* (2018) Protective mechanisms of butyrate on inflammatory bowel disease. Curr Pharm Des 24(35):4154–4166

13. Couch DG, Tasker C, Theophilidou E, Lund JN, O'Sullivan SE (2017) Cannabidiol and palmitoylethanolamide are anti-inflammatory in the acutely inflamed human colon. Clin Sci (Lond) 1;131(21):2611–2626

14. Petrosino S, Schiano Moriello A, Verde R, Allarà M, Imperatore R, Ligresti A, *et al* (2019) Palmitoylethanolamide counteracts substance P-induced mast cell activation in vitro by stimulating diacylglycerol lipase activity. J Neuroinflammation 16(1):274

15. Lang-Illievich K, Klivinyi C, Lasser C, Brenna CTA, Szilagyi IS, Bornemann-Cimenti H (2023) Palmitoylethanolamide in the treatment of chronic pain: a systematic review and meta-analysis of double-blind randomized controlled trials. Nutrients 15(6):1350

16. Nau R, Ribes S, Djukic M, Eiffert H (2014) Strategies to increase the activity of microglia as efficient protectors of the brain against infections. Front Cell Neurosci 8:138

17. D'Agostino G, Russo R, Avagliano C, Cristiano C, Meli R, Calignano A (2012) Palmitoylethanolamide protects against the amyloid-β25-35-induced learning and memory impairment in mice, an experimental model of Alzheimer disease. Neuropsychopharmacology 37(7):1784–1792

18. Borrelli F, Romano B, Petrosino S, Pagano E, Capasso R, Coppola D, *et al* (2015) Palmitoylethanolamide, a naturally occurring lipid, is an orally effective intestinal anti-inflammatory agent. Br J Pharmacol 172(1):142–158

19. Clayton P, Hill M, Bogoda N, Subah S, Venkatesh R (2021) Palmitoylethanolamide: A natural compound for health management. Int J Mol Sci 22(10):5305

20. Skaper SD, Facci L, Giusti P (2014) Mast cells, glia and neuroinflammation: partners in crime? Immunology 141(3):314–327

21. Gugliandolo E, Peritore A, Piras C, Cuzzocrea S, Crupi R (2020) Palmitoylethanolamide and related ALIAmides: prohomeostatic lipid compounds for animal health and wellbeing. Vet Sci 7(2):78

22. Hauer D, Schelling G, Gola H, Campolongo P, Morath J, Roozendaal B, *et al* (2013) Plasma concentrations of endocannabinoids and related primary fatty acid amides in patients with post-traumatic stress disorder. PLoS One 8(5):e62741

23. Snider AJ *et al* (2009) A role for sphingosine kinase 1 in dextran sulfate sodium-induced colitis. FASEB J 23(1) 143–152

24. Rose WA, Sakamoto K, Leifer CA (2012), Multifunctional role of dextran sulfate sodium for in vivo modeling of intestinal diseases. BMC Immunol 13(1):41

25. Samak G, Chaudhry KK, Gangwar R, Narayanan D, Jaggar JH, Rao R (2015) Calcium/Ask1/MKK7/JNK2/c-Src signalling cascade mediates disruption of intestinal epithelial tight junctions by dextran sulfate sodium. Biochem J 465(3):503–515

26. Araki Y, Sugihara H, Hattori T (2006) In vitro effects of dextran sulfate sodium on a Caco-2 cell line and plausible mechanisms for dextran sulfate sodium-induced colitis. Oncol Rep 16(6):1357–1362

27. Ye Z, Mishchuk DO, Stephens NS, Slupsky CM (2011) Dextran sulfate sodium inhibits alanine synthesis in Caco-2 cells. Int J Mol Sci 12(4):2325–2335

28. Roselli M, Maruszak A, Grimaldi R, Harthoorn L, Finamore A (2022) Galactooligosaccharide. Front Nutr 9:862974

29. Hung T Van, Suzuki T (2018) Short-chain fatty acids suppress inflammatory reactions in caco-2 cells and mouse colons. J Agric Food Chem 66(1):108–117

30. Zheng L, Kelly CJ, Battista KD, Schaefer R, Lanis JM, Alexeev EE, *et al* (2017) Microbial-derived butyrate promotes epithelial barrier function through IL-10 receptor-dependent repression of Claudin-2. J Immunol 199(8):2976–2984

31. Magnusson MK, Isaksson S, Öhman L (2020) The anti-inflammatory immune regulation induced by butyrate is impaired in inflamed intestinal mucosa from patients with ulcerative colitis. Inflammation 43(2):507–517

32. Kim JJ, Shajib MS, Manocha MM, Khan WI (2012). Investigating intestinal inflammation in DSS-induced Model of IBD. J Vis Exp (60):3678

33. Rubio CA, Schmidt PT, Lang-Schwarz C, Vieth M (2022) Branching crypts in inflammatory bowel disease revisited. J Gastroenterol Hepatol 37(3):440–445

34. Gasaly N, Hermoso MA, Gotteland M (2021) Butyrate and the fine-tuning of colonic homeostasis: implication for inflammatory bowel diseases. Int J Mol Sci 22(6):3061

35. Wright K, Rooney N, Feeney M, Tate J, Robertson D, Welham M, *et al* (2005) Differential expression of cannabinoid receptors in the human colon: cannabinoids promote epithelial wound healing. Gastroenterology 129(2):437–453

36. Thanabalasuriar A, Koutsouris A, Weflen A, Mimee M, Hecht G, Gruenheid S (2010) The bacterial virulence factor NleA is required for the disruption of intestinal tight junctions by enteropathogenic Escherichia coli. Cell Microbiol 12(1):31–41

37. Tong J, Wang Y, Chang B, Zhang D, Wang B (2013) Evidence for the involvement of RhoA signaling in the ethanol-induced increase in intestinal epithelial barrier permeability. Int J Mol Sci 14(2):3946–3960

38. Capaldo CT, Farkas AE, Hilgarth RS, Krug SM, Wolf MF, Benedik JK, *et al* (2014) Proinflammatory cytokine-induced tight junction remodeling through dynamic self-assembly of claudins. Mol Biol Cell 25(18):2710–2719

39. Al-Sadi RM, Ma TY (2007) IL-1β Causes an increase in intestinal epithelial tight junction permeability. J Immunol 178(7):4641–4649

40. Bai B, Li H, Han L, Mei Y, Hu C, Mei Q, *et al* (2022) Molecular mechanism of the TGF-β/Smad7 signaling pathway in ulcerative colitis. Mol Med Rep 25(4):116

41. Poritz LS, Garver KI, Green C, Fitzpatrick L, Ruggiero F, Koltun WA (2007). Loss of the tight junction protein ZO-1 in dextran sulfate sodium induced colitis. J Surg Res 140(1):12–19

42. Zhao Q, Liu Y, Tan L, Yan L, Zuo X (2018) Adiponectin administration alleviates DSS-induced colonic inflammation in Caco-2 cells and mice. Inflamm Res 67(8):663–670

43. Zhao H, Yan R, Zhou X, Ji F, Zhang B (2016) Hydrogen sulfide improves colonic barrier integrity in DSS-induced inflammation in Caco-2 cells and mice. Int Immunopharmacol 39:121–127

44. Wächtershäuser A, Loitsch SM, Stein J (2000) PPAR-gamma is selectively upregulated in Caco-2 cells by butyrate. Biochem Biophys Res Commun 272(2):380–385

45. Paterniti I, Impellizzeri D, Crupi R, Morabito R, Campolo M, Esposito E, *et al* (2013) Molecular evidence for the involvement of PPAR-δ and PPAR-γ in anti-inflammatory and neuroprotective activities of palmitoylethanolamide after spinal cord trauma. J Neuroinflammation 10(1):787

46. Petrosino S, Schiano Moriello A, Cerrato S, Fusco M, Puigdemont A, De Petrocellis L, *et al* (2016) The anti-inflammatory mediator palmitoylethanolamide enhances the levels of 2-arachidonoyl-glycerol and potentiates its actions at TRPV1 cation channels. Br J Pharmacol 173(7):1154–1162

47. Ambrosino P, Soldovieri MV, Russo C, Taglialatela M (2013) Activation and desensitization of TRPV1 channels in sensory neurons by the PPARα agonist palmitoylethanolamide. Br J Pharmacol 168(6):1430–1444

48. Karwad MA, Couch DG, Wright KL, Tufarelli C, Larvin M, Lund J, *et al* (2019) Endocannabinoids and endocannabinoid-like compounds modulate hypoxia-induced permeability in CaCo-2 cells via CB1, TRPV1, and PPARα. Biochem Pharmacol 168:465–472

49. Bonomo RR, Cook TM, Gavini CK, White CR, Jones JR, Bovo E, *et al* (2020). Fecal transplantation and butyrate improve neuropathic pain, modify immune cell profile, and gene expression in the PNS of obese mice. Proc Natl Acad Sci 117(42):26482–26493